

Unsupervised Multi-Modality Registration Network based on Spatially Encoded Gradient Information

Wangbin Ding¹, Lei Li^{2,3}, Xiahai Zhuang^{2,*}, and Liqin Huang^{1,*}

¹ College of Physics and Information Engineering, Fuzhou University, Fuzhou, China

² School of Data Science, Fudan University, Shanghai, China

³ School of Biomedical Engineering, Shanghai Jiao Tong University, Shanghai, China

Abstract. Multi-modality medical images can provide relevant and complementary anatomical information for a target (organ, tumor or tissue). Registering the multi-modality images to a common space can fuse these comprehensive information, and bring convenience for clinical application. Recently, neural networks have been widely investigated to boost registration methods. However, it is still challenging to develop a multi-modality registration network due to the lack of robust criteria for network training. Besides, most existing registration networks mainly focus on pairwise registration, and can hardly be applicable for multiple image scenarios. In this work, we propose a multi-modality registration network (MMRegNet), which can jointly register multiple images with different modalities to a target image. Meanwhile, we present spatially encoded gradient information to train the MMRegNet in an unsupervised manner. The proposed network was evaluated on two datasets, i.e, MM-WHS 2017 and CHAOS 2019. The results show that the proposed network can achieve promising performance for cardiac left ventricle and liver registration tasks. Source code is released publicly on github⁴.

Keywords: Multi-Modality Registration · Gradient Information · Unsupervised Registration Network.

1 Introduction

Registration is a critical technology to establish correspondences between medical images [8]. The study of registration algorithm enables tumor monitoring [16], image-guided intervention [1], and treatment planning [6]. Multi-modality images, such as CT, MR and US, capture different anatomical information. Alignment of the multi-modality images can help a clinician to improve the disease diagnosis and treatment [5]. For instance, Zhuang [20] registered multi-modality myocardium MR images to fuse complementary information for myocardial segmentation and scar quantification. Heinrich et al. [9] performed registration of intra-operative US to pre-operative MR, which could aid image-guided neurosurgery.

⁴ <https://github.com/NanYoMy/mmregnet>

Over the last decades, various methods have been proposed to perform multi-modality image registration. The most common methods are based on statistical similarity metric, such as MI [14], NMI[17] and SEMI [21]. Registrations are performed by maximizing these similarity metrics between the moved image and the fixed image. Whereas these metrics usually suffer from the loss of spatial information [15]. Other common methods are based on invariant representation. Wachinger et al. [18] presented the entropy and Laplacian image which are invariant structural representations across the multi-modality image, and registrations were achieved by minimizing the difference between the invariant representations. Zhuang et al. [22] proposed the normal vector information of intensity image for registration, which obtained comparable performance to the MI and NMI. Furthermore, Heinrich et al. [8] designed a handcraft modality independent neighborhood descriptor to extract structure information for registrations. Nevertheless, these conventional methods solved the registration problem by iterative optimizing, which is not applicable for time-sensitive scenarios.

Recently, several registration networks, which could efficiently achieve registrations in an one-step fashion, have been widely investigated. Hu et al. [10] proposed a weakly supervised registration neural network for multi-modality images. They utilized anatomical labels as the criteria for network training. Similarly, Balakrishnan et al. [4] proposed a learning-based framework for image registration. The framework could extend to multi-modality images when the anatomical label is provided during the training. Furthermore, Luo et al. [13] proposed a group-wise registration network, which could jointly register multiple atlases to a target image. Still, these methods required extensive anatomical labels for network training, which prevents them from unlabeled datasets.

At present, based on image-to-image translation generative adversarial network (GAN) [11], several unsupervised registration networks had been proposed. Qin et al. [15] disentangled a shape representation from multi-modality images via GAN, then a convenient mono-modality similarity metric could be applied on the shape representation for registration network training. Arar et al. [2] connected registration network with a style translator. The network could jointly perform spatial and style transformation on a moving image, and was trained by minimizing the difference between the transformed moving image and the fixed image. The basic idea of these GAN-based methods is converting the multi-modality registration problem into a mono-modality one. Unfortunately, GAN methods easily cause geometrical distortions and intensity artifacts during image translation [19], which may lead to unrealistic registration results. Furthermore, existing networks mainly focus on pair-wise registration, and hardly explore the multi-modality multi-image registration problem.

In this work, we propose an end-to-end multi-modality registration network (MMRegNet). The main contributions are: (1) We propose a new registration network, which could jointly register multiple images with different modalities to a target image. (2) We present a spatially encoded gradient information (SEGI), which can provide a similarity criteria to train the registration network in an

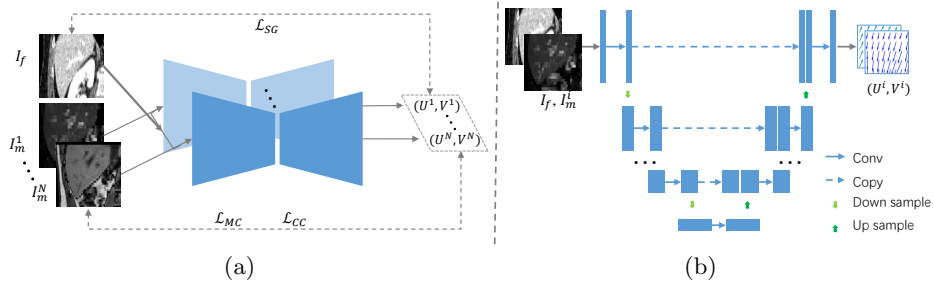


Fig. 1. The overview of the proposed MMRegNet. (a) the overall architecture of the MMRegNet; (b) the sub-registration network in the MMRegNet. Please see the github for implementation details

unsupervised manner. (3) We evaluated our method on multi-modality cardiac left ventricle and liver registration tasks, and it achieved promising performance on both applications.

2 Method

Network Architecture: The MMRegNet aims to jointly register multiple images to a target image. Let $\mathcal{I} = \{I_m^i | i = 1 \dots N\}$ be a set of moving images where each image was acquired via different imaging protocol, and I_f be a fixed image. I_m^i and I_f are defined in a 3-D spatial domain Ω . The MMRegNet is designed to simultaneously predict forward U^i and backward V^i dense displacement fields (DDFs) between each pair of I_m^i and I_f . Totally, it can produce N pairs of DDFs between \mathcal{I} and I_f ,

$$\{(U^i, V^i) | i = 1 \dots N\} = f_\theta(\mathcal{I}, I_f) \quad (1)$$

where θ is the parameter of the MMRegNet. For convenience, we abbreviate I_m^i , U^i and V^i as I_m , U and V when no confusion is caused. Each voxel $x \in \Omega$ in I_m and I_f can be transformed by U and V as follows,

$$(I_m \circ U)(x) = I_m(x + U(x)), \quad (2)$$

$$(I_f \circ V)(x) = I_f(x + V(x)), \quad (3)$$

where $I_m \circ U$ and $I_f \circ V$ denote the moved image of I_m and I_f , respectively.

Figure 1 (a) shows the overall architecture of the MMRegNet, it is composed of N sub-registration networks. As shown in Figure 1 (b), each sub-registration network contains four downsample and four upsample operations, and outputs forward and backward DDFs for an inputted image pair. In this way, the MMRegNet can jointly register multiple different modality of moving images to a target.

Spatially Encoded Gradient Information: Generally, the parameter of MMRegNet could be optimized by minimizing the intensity-based criteria, such as mean square error of intensity, between the moved image and fixed image. However, such metrics are ill-posed when applied in multi-modality scenarios. This is because the intensity distribution of an anatomy usually varies across different modality images. Therefore, we adapt normalized gradient information (NGI) [7] to train the network. The idea of NGI is based on the assumption that image

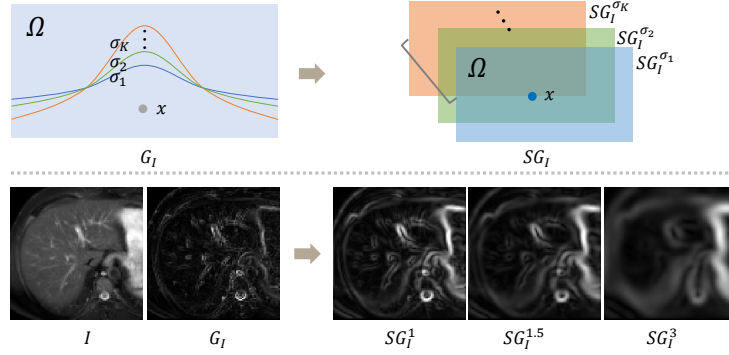


Fig. 2. The visual demonstration of the SEGI. The upper panel illustrates the basic idea of the SEGI. The lower panel presents a representative T2 liver image (I), as well as its corresponding normalized gradient (G_I) and spatially encoded gradient ($SG_I^1, SG_I^{1.5}, SG_I^3$) images.

structures can be defined by intensity changes. Let G_I be the NGI of an intensity image I , each element of G_I is calculated as follows,

$$G_I(x) = \frac{\nabla I(x)}{\|\nabla I(x)\|_2}, \quad (4)$$

where $x \in \Omega$, ∇I refers to the gradient of image I . Ideally, the MMRegNet can be trained by minimizing the difference between the $G_{I_m \circ U}$ and G_{I_f} . However, such a metric could be easily affected by the noises or artifacts of the intensity image. To overcome this, we extend the NGI to the SEGI. The upper panel of Figure 2 illustrates the idea of SEGI, it is achieved by introducing a set of spatial variables $\Sigma = \{\sigma_1, \sigma_2, \dots, \sigma_K\}$ to the standard NGI (G_I). For each spatial variables σ_k , we compute its associated SEGI ($SG_I^{\sigma_k}$) as follows,

$$SG_I^{\sigma_k}(x) = \sum_{p \in \Omega} \mathcal{N}(p|x, \sigma_k^2) \frac{|\nabla I(p)|}{\|\nabla I(p)\|_2}, \quad (5)$$

where $x \in \Omega$, $\mathcal{N}(p|x, \sigma_k^2)$ denotes Gaussian distribution. Notably, we weighted accumulate gradient information around x , which results in a more robust representation of the intensity change (see the lower panel of Figure 2). Finally, given

the whole set of spatial variables Σ , the SEGI of an intensity image I is defined as,

$$SG_I = \{SG_I^{\sigma_1}, SG_I^{\sigma_2}, \dots, SG_I^{\sigma_K}\}. \quad (6)$$

Loss Function: We train the network by minimizing the cosine distance between the SEGI of each moved image $(SG_{I_m \circ U})$ and fixed image (SG_{I_f}) ,

$$\mathcal{L}_{SG} = \frac{1}{N \times K} \sum_{i=1}^N \sum_{k=1}^K \mathcal{D}(SG_{I_m^i \circ U^i}^{\sigma_k}, SG_{I_f}^{\sigma_k}), \quad (7)$$

$$\mathcal{D}(SG_{I_m^i \circ U^i}^{\sigma_k}, SG_{I_f}^{\sigma_k}) = \frac{-1}{|\Omega|} \sum_{x \in \Omega} \cos(SG_{I_m^i \circ U^i}^{\sigma_k}(x), SG_{I_f}^{\sigma_k}(x)), \quad (8)$$

where $|\Omega|$ counts the number of voxels in an image, $\cos(\mathbf{A}, \mathbf{B})$ calculates the cosine distance between vector \mathbf{A} and \mathbf{B} .

Meanwhile, the MMRegNet is designed to simultaneously predict U and V for each pair of I_m and I_f . Normally, the U and V should be inverse of each other. Hence, we introduce a cycle consistent constraint for the DDFs such that each I_m can be restored to its original one after transforming by U and V in succession,

$$\mathcal{L}_{CC} = \frac{1}{N \times |\Omega|} \sum_{i=1}^N \sum_{x \in \Omega} \|I_m^i \circ U^i \circ V^i(x) - I_m^i(x)\|_1. \quad (9)$$

Moreover, the MMRegNet jointly register multiple I_m to a same target I_f . Ideally, all the $I_m \circ U$ should be aligned to have the same spatial structure. Therefore, we further introduce a move consistent loss to minimize the SEGI difference among the moved images as follows,

$$\mathcal{L}_{MC} = \frac{1}{N^2 \times K} \sum_{i=1}^N \sum_{j=1}^N \sum_{k=1}^K \mathcal{D}(SG_{I_m^i \circ U^i}^{\sigma_k}, SG_{I_m^j \circ U^j}^{\sigma_k}). \quad (10)$$

Finally, the total trainable loss of the registration network is defined as follows,

$$\mathcal{L} = \mathcal{L}_{SG} + \lambda_1 \mathcal{L}_{CC} + \lambda_2 \mathcal{L}_{MC} + \frac{\lambda_3}{2 \times N} \sum_{i=1}^N \{\Psi(U^i) + \Psi(V^i)\}. \quad (11)$$

where $\Psi(U^i)$ and $\Psi(V^i)$ are smoothness regularization terms for DDFs, λ_1 , λ_2 and λ_3 are the hyper-parameters.

3 Experiments and Results

Experimental Setups: The MMRegNet was implemented by the TensorFlow on an NVIDIA P100. The spatial variables Σ was given to $\{1, 1.5, 3\}$, while the λ_1 , λ_2 and λ_3 (see Eq.11) were set to 0.1, 0.01 and 10, respectively. The ADAM

Table 1. The performance of different multi-modality registration methods on MM-WHS dataset.

Method	LVC (MR→CT)		Myo (MR→CT)	
	DS (%)↑	ASD (mm)↓	DS (%)↑	ASD (mm)↓
Sy-NCC [3]	70.07±16.57	4.51±2.67	50.66±16.02	4.10±1.77
Sy-MI [3]	69.16±15.25	4.66±2.54	49.00±16.21	4.34±2.04
VM-NCC [4]	79.46±8.73	2.81±1.05	62.77±9.51	2.49±0.61
MMRegNet	81.24±7.77	2.96±0.95	64.68±7.98	2.77±0.53

optimizer was employed to train the MMRegNet for two public datasets, i.e., the MM-WHS⁵ [23] and CHAOS⁶ [12].

- MM-WHS: The MM-WHS contains multi-modality (CT, MR) cardiac medical images. We utilized 20 MR and 20 CT images for left ventricle registration. The MMRegNet was trained to perform the registration of MR to CT images. Note that the number of modalities in \mathcal{I} is equal to one in this task, thus the MMRegNet degenerated to a pair-wise registration network.
- CHAOS: The CHAOS contains multi-modality abdominal images from healthy volunteers. For each volunteer, the dataset includes their T1, T2 and CT images. We adopted 20 T1 MR, 20 T2 MR and 20 CT images for liver registration. The MMRegNet was trained to jointly register T1 and T2 images to CT images.

To evaluate the performance of the registration network, we computed the Dice (DS) and average symmetric surface distance (ASD) between the corresponding label of moved and fixed image. Meanwhile, all the experimental results were reported by 4-fold cross-validation.

Results: We compared our registration method with three state-of-the-art multi-modality registration methods.

- Sy-NCC: The conventional affine + deformable registration, which is based on the symmetric image normalization method with normalized cross-correlation (NCC) as optimization metric [3]. We implemented it based on the popular ANTs software package⁷ .
- Sy-MI: The Sy-NCC method which uses the MI instead of the NCC as optimization metric.
- VM-NCC: The state-of-the-art pair-wise registration network [4], which was trained by using the NCC as training criteria. We adopted their official online implementation⁸.

Table 1 shows the results on MM-WHS dataset. Compared with the conventional methods (Sy-NCC and Sy-MI), the MMRegNet could achieve better

⁵ www.sdspeople.fudan.edu.cn/zhuangxiahai/0/mmwchs/

⁶ <https://chaos.grand-challenge.org/>

⁷ <https://github.com/ANTsX/ANTsPy>

⁸ <https://github.com/voxelmorph/voxelmorph>

Table 2. The performance of different multi-modality registration methods on CHAOS dataset.

Method	Liver (T1→CT)		Liver (T2→CT)	
	DS (%)↑	ASD (mm)↓	DS (%)↑	ASD (mm)↓
Sy-NCC [3]	74.94±11.05	8.46±4.10	75.46±9.42	8.41±3.86
Sy-MI [3]	73.88±10.08	8.84±3.70	75.82±7.23	8.32±2.73
VM-NCC [4]	74.63±6.54	8.25±2.17	71.10±6.09	9.30±2.01
MMRegNet	78.28±5.85	7.09±1.77	77.98±5.65	7.60±1.65

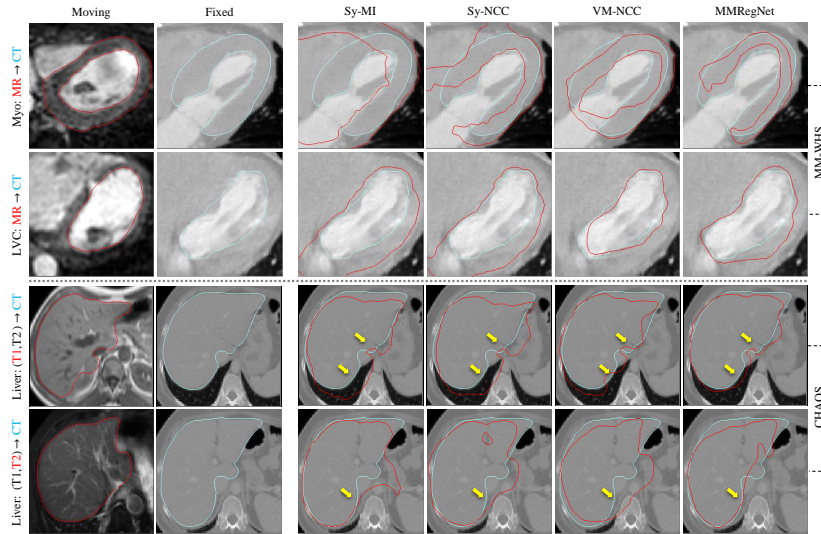


Fig. 3. Visualization of different methods on MM-WHS and CHAOS datasets. The showed images are the median cases in terms of DS by the MMRegNet. The blue contours are the gold standard label of the fixed images, while the red contours delineate the label of moving or moved images. The yellow arrows indicate the advantage of the MMRegNet. (The reader is referred to the online version of this article)

performance on both left ventricle cavity (LVC) and left ventricle myocardium (Myo). Notably, compared to the state-of-the-art pair-wise registration network, i.e., VM-NCC, the MMRegNet obtained comparable results in terms of DS and ASD. This reveals that the MMRegNet is also applicable for pair-wise registration tasks, and the proposed SEGI could serve as another efficient metric, such as MI and NCC, for multi-modality registration.

Table 2 shows the results on CHAOS dataset. The Sy-NCC, Sy-MI, and VM-NCC are originally designed for pair-wise registration. For these methods, we independently conducted the registration of T1 or T2 to CT images. For the MMRegNet, we jointly registered T1 and T2 to the CT images. The MMRegNet obtained average 5.27 % (p-value < 0.01) and 1.43 mm (p-value < 0.01) improvements against VM-NCC in terms of DS and ASD, respectively. Meanwhile, the MMRegNet achieved comparable accuracy to the state-of-the-art conven-

tional methods, i.e., Sy-MI and Sy-NCC. This demonstrates that the MMRegNet could achieve promising performance for multi-modality multi-image registration tasks.

Additionally, Figure 3 visualizes four representative cases from the two datasets. For the MM-WHS dataset, one can observe that both the VM-NCC and MMRegNet achieved better visual results than the Sy-MI and Sy-NCC, which is consistent with the quantitative results in Table 1. For the CHAOS dataset, the yellow arrows highlight that the MMRegNet could obtain more reasonable details than other methods.

Furthermore, we deeply investigated the effectiveness of the SEGI. As Figure 4 (a) shows, we first prepared a pair of pre-aligned T1 and CT images. Then, we applied rigid translations to the T1 image along the axial direction. Figure 4 (b) tracks the corresponding value of three metrics, i.e., SEGI difference (see Eq. 8), negative MI and negative NCC, between the transformed T1 and the CT images. One can observe that NCC curve contains a local minimal region (Arrow (1)), and the MI curve may easily suffer from gradient vanishes in the flatten areas (Arrow (2)), whereas the SEGI curves exhibit robust performance. This reveals that the SEGI could provide efficient criteria for gradient-based optimizers.

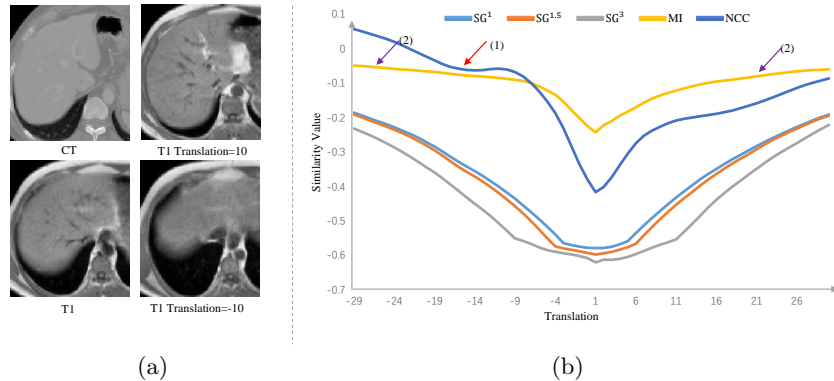


Fig. 4. The trace of different metrics against the translations. (a) the manually pre-aligned T1 and CT, as well as two transformed T1 images. (b) the values of the SEGI difference (SG^1 , $SG^{1.5}$, SG^3), negative MI and negative NCC with respect to the translations (in range $[-30, 30]$).

4 Conclusion

In this paper, we propose an end-to-end network for multi-modality registration. The network is both applicable for pair-wise image registration and multiple image registration tasks. In the network, we present the SEGI which could obtain a robust structural representation for multi-modality images. Effectively, the

SEGI could be applied as the loss function for unsupervised registration network training. The results show that the MMRegNet achieved promising performance when comparing with the state-of-the-art registration methods. Further work will extend the MMRegNet to other multi-modality datasets.

References

1. Alam, F., Rahman, S.U., Ullah, S., Gulati, K.: Medical image registration in image guided surgery: Issues, challenges and research opportunities. *Biocybernetics and Biomedical Engineering* **38**(1), 71–89 (2018)
2. Arar, M., Ginger, Y., Danon, D., Bermano, A.H., Cohen-Or, D.: Unsupervised multi-modal image registration via geometry preserving image-to-image translation. In: Proceedings of the IEEE/CVF conference on computer vision and pattern recognition. pp. 13410–13419 (2020)
3. Avants, B.B., Tustison, N., Song, G.: Advanced normalization tools (ANTS). *Insight j* **2**(365), 1–35 (2009)
4. Balakrishnan, G., Zhao, A., Sabuncu, M.R., Guttag, J., Dalca, A.V.: Voxelmorph: a learning framework for deformable medical image registration. *IEEE transactions on medical imaging* **38**(8), 1788–1800 (2019)
5. Fu, Y., Lei, Y., Wang, T., Curran, W.J., Liu, T., Yang, X.: Deep learning in medical image registration: a review. *Physics in Medicine & Biology* **65**(20), 20TR01 (2020)
6. Giesel, F., Mehndiratta, A., Locklin, J., McAuliffe, M., White, S., Choyke, P., Knopp, M., Wood, B., Haberkorn, U., von Tengg-Kobligk, H.: Image fusion using ct, mri and pet for treatment planning, navigation and follow up in percutaneous rfa. *Experimental oncology* **31**(2), 106 (2009)
7. Haber, E., Modersitzki, J.: Intensity gradient based registration and fusion of multi-modal images. In: International Conference on Medical Image Computing and Computer-Assisted Intervention. pp. 726–733. Springer (2006)
8. Heinrich, M.P., Jenkinson, M., Bhushan, M., Matin, T., Gleeson, F.V., Brady, M., Schnabel, J.A.: MIND: Modality independent neighbourhood descriptor for multi-modal deformable registration. *Medical image analysis* **16**(7), 1423–1435 (2012)
9. Heinrich, M.P., Jenkinson, M., Papiez, B.W., Brady, M., Schnabel, J.A.: Towards realtime multimodal fusion for image-guided interventions using self-similarities. In: International conference on medical image computing and computer-assisted intervention. pp. 187–194. Springer (2013)
10. Hu, Y., Modat, M., Gibson, E., Li, W., Ghavami, N., Bonmati, E., Wang, G., Bandula, S., Moore, C.M., Emberton, M., et al.: Weakly-supervised convolutional neural networks for multimodal image registration. *Medical image analysis* **49**, 1–13 (2018)
11. Huang, X., Liu, M.Y., Belongie, S., Kautz, J.: Multimodal unsupervised image-to-image translation. In: Proceedings of the European conference on computer vision (ECCV). pp. 172–189 (2018)
12. Kavur, A.E., Gezer, N.S., Bariş, M., Aslan, S., Conze, P.H., Groza, V., Pham, D.D., Chatterjee, S., Ernst, P., Ozkan, S., et al.: CHAOS challenge-combined (CT-MR) healthy abdominal organ segmentation. *Medical Image Analysis* **69**, 101950 (2021)
13. Luo, X., Zhuang, X.: Mvmm-regnet: A new image registration framework based on multivariate mixture model and neural network estimation. In: International Conference on Medical Image Computing and Computer-Assisted Intervention. pp. 149–159. Springer (2020)

14. Maes, F., Collignon, A., Vandermeulen, D., Marchal, G., Suetens, P.: Multimodality image registration by maximization of mutual information. *IEEE transactions on Medical Imaging* **16**(2), 187–198 (1997)
15. Qin, C., Shi, B., Liao, R., Mansi, T., Rueckert, D., Kamen, A.: Unsupervised deformable registration for multi-modal images via disentangled representations. In: *International Conference on Information Processing in Medical Imaging*. pp. 249–261. Springer (2019)
16. Seeley, E.H., Wilson, K.J., Yankeelov, T.E., Johnson, R.W., Gore, J.C., Caprioli, R.M., Matrisian, L.M., Sterling, J.A.: Co-registration of multi-modality imaging allows for comprehensive analysis of tumor-induced bone disease. *Bone* **61**, 208–216 (2014)
17. Studholme, C., Hill, D.L., Hawkes, D.J.: An overlap invariant entropy measure of 3D medical image alignment. *Pattern recognition* **32**(1), 71–86 (1999)
18. Wachinger, C., Navab, N.: Entropy and laplacian images: Structural representations for multi-modal registration. *Medical image analysis* **16**(1), 1–17 (2012)
19. Zhang, Z., Yang, L., Zheng, Y.: Translating and segmenting multimodal medical volumes with cycle-and shape-consistency generative adversarial network. In: *Proceedings of the IEEE conference on computer vision and pattern Recognition*. pp. 9242–9251 (2018)
20. Zhuang, X.: Multivariate mixture model for myocardial segmentation combining multi-source images. *IEEE transactions on pattern analysis and machine intelligence* **41**(12), 2933–2946 (2018)
21. Zhuang, X., Arridge, S., Hawkes, D.J., Ourselin, S.: A nonrigid registration framework using spatially encoded mutual information and free-form deformations. *IEEE transactions on medical imaging* **30**(10), 1819–1828 (2011)
22. Zhuang, X., Gu, L., Xu, J.: Medical image alignment by normal vector information. In: *International Conference on Computational and Information Science*. pp. 890–895. Springer (2005)
23. Zhuang, X., Li, L., Payer, C., Štern, D., Urschler, M., Heinrich, M.P., Oster, J., Wang, C., Smedby, Ö., Bian, C., et al.: Evaluation of algorithms for multi-modality whole heart segmentation: an open-access grand challenge. *Medical image analysis* **58**, 101537 (2019)